NANO LETTERS

2006
Vol. 6, No. 2
296−300

Controlling Nanowear in a Polymer by Confining Segmental Relaxation

Bernd Gotsmann* and Urs T. Duerig

IBM Research GmbH, Zurich Research Laboratory, 8803 Rüschlikon, Switzerland

Scott Sills, Jane Frommer, and Craig J. Hawker†

IBM Research, Almaden Research Center, 650 Harry Road, San Jose, California 95120

Received October 17, 2005

ABSTRACT

Molecular relaxation of a copolymer designed for nano-electromechanical systems was chemically confined by varying the spacing between cross-links, δ_c. A critical cross-link spacing of 1–3 nm marks a transition in the nano-mechanical properties evaluated by atomic force microscopy. The transition reveals an interplay between the cross-link spacing and the length scale for backbone relaxation, ξ_α, in cooperatively rearranging regions. For $\delta_c \gg \xi_\alpha$, the natural backbone relaxation process is relatively unaffected by the cross-links and a ductile, low hardness behavior results. For $\delta_c < \xi_\alpha$, the cross-links directly interfere with backbone relaxation and confine segmental mobility, leading to a brittle, high hardness response.

Nano-electromechanical systems (NEMS) are receiving considerable attention in both science and technology. Friction and wear are among the most critical problems to be solved in order to fabricate commercially viable devices with moving parts.[1] Extensive efforts have been devoted to controlling and minimizing wear. However, when device applications require nanoscale phase homogeneity, specialty coatings, composite reinforcement, and third body lubrication become unattractive approaches to tackling wear issues. Examples of such applications include scanned-probe data storage[2,3] and scanned-probe lithography and patterning.[4]

Wear management in NEMS must evolve from the molecular scale. Macroscopic wear phenomenology, with descriptors such as yield stress, hardness, wear volume, etc., fails to completely describe molecular and nanoscale wear processes. Nanoscopic wear characteristics of polymers are regulated by the interaction of critical molecular length scales, including relaxation length scales, the spacing between cross-links, and the size of external contacts.

Many proposed NEMS schemes incorporate sharp probes for transport, sensing, and patterning operations. Under loading forces of a few nanonewtons, a nanometer sharp tip typically produces stresses of hundreds of megapascals. A polymer surface beneath the tip accommodates these stresses through both viscoelastic and plastic modes. The frictional energy is dissipated either internally, i.e., through viscoelastic molecular relaxation processes,[5−7] or through pseudoplastic mechanisms such as chain pull-out, scission,[8] or crazing.[9] The wear characteristics of the surface inevitably depend on which relaxation modes are available under the sliding conditions and on the extent to which the relaxation processes are spatially correlated throughout the material.

In this Letter, we focus on controlling the wear characteristics of synthetic polymers for contact mechanical operations in NEMS. By reducing the cross-link spacing, we confine natural molecular relaxation and reveal a transition between the dominant wear mechanism: from viscoelastic rippling in a ductile material to pseudoplastic, abrasive wear in a brittle material. The transition between wear modes occurs when the spacing between cross-links matches the length scale required for segmental backbone relaxation.

Random copolymers of styrene and benzocyclobutene (PS−BCB)[10] were selected as a model system, based on the developing technology of scanned-probe data storage.[2,3] Latent cross-links are provided via the BCB groups, with the primary reaction pathway proposed in Figure 1:

PS−BCB films (20 nm thick) were spin cast from cyclohexanone solutions (1 wt %) onto silicon wafers coated with an epoxy (SU8) buffer layer (80 nm). The buffer serves to prevent tip wear if penetration through the surface film occurs. The films were thermally cross-linked under nitrogen at 220 °C for 1 h.[10] The BCB content was varied during synthesis from 0 to 30 mol %, with overall molecular weights M_w and molecular weight between cross-links M_c ranging from 14 to 123 kDa and 243−17400 Da, respectively.[11] The

* Corresponding author, bgo@zurich.ibm.com.
† Present address: University of California, Santa Barbara, CA 93106-9510.

10.1021/nl0520563 CCC: $33.50
Published on Web 01/11/2006

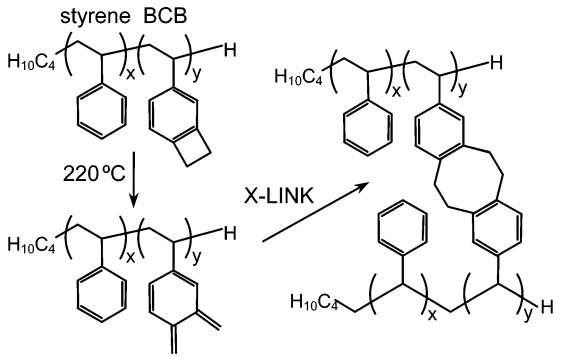

Figure 1. A cross-linking mechanism for random styrene−benzocyclobutene copolymers (PS−BCB), with a BCB content (y) varying between 0 and 30%.

molecular weight between cross-links was determined by $M_c = M_S(1 - x)/x$, with the styrene weight $M_S = 104$ Da and $x =$ the mole fraction of styrene.[11]

Wear experiments were performed on the PS−BCB films with an atomic force microscope (AFM) and a cantilevered tip (20−30 nm diameter hemisphere), both custom made. An area of $(2.5\ \mu m)^2$ was scanned in 512 lines at 50 μm/s in a saw-tooth pattern, with a constant applied load of 2−5 nN. After a prescribed number of scans, the worn and surrounding areas were imaged for wear analysis with the same tip in thermoelectric topographic imaging mode.[2] In all cases, the sample temperature remained below the glass transition.

We observe a variety of nanowear modes (Figure 2). For an un-cross-linked polymer, wear typically begins as a ripple pattern[5,14−17] after only a few scans (Figure 2a). Ripple wear is a viscoelastic process where material is displaced from its original position yet remains within the continuum of its environment. The displaced material does not spontaneously relax to its original position because of energy losses due to viscous dissipation, i.e., internal friction. Relaxation due to surface tension, residual stresses, or entropic driving forces does not occur on the time scale of the experiments because the relaxation dynamics are very slow below T_g. The possibility for modified relaxation dynamics in a sub-nanometer *mobile surface layer* is negligible considering a ripple amplitude that ranges from 10 to 20 nm. The initial rippling remains fairly stable for tens to hundreds of scans before the surface is finally torn apart through pseudoplastic modes that *remove* material from the continuum of its environment as a debris particle (Figure 2b). For more highly cross-linked materials, initial ripple formation is suppressed, and surface tearing and abrasion are only seen after hundreds to thousands of scans (parts c and d of Figure 2). Finally, the different wear modes should not be regarded as independent of each other; they can change with time, applied load, and cross-link density.

Finding a suitable way to quantify wear has always been a challenge in wear analysis. Classical approaches include scratch or indentation resistance.[12,13] However, these do not allow distinguishing between the different wear modes observed nanoscopically. In addition, the common measure of *wear volume* is inadequate for nanowear because material may be *displaced* from its original position, but not always

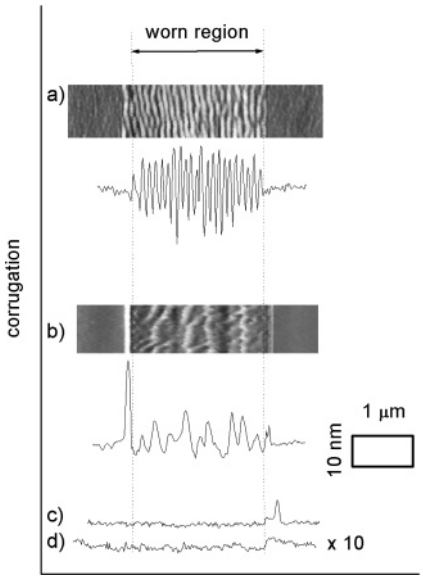

Figure 2. Wear patterns on PS−BCB surfaces with different cross-link densities: (a) un-cross-linked, PS, ripple formation after 4 scans (also observed on low cross-link density samples); (b) cross-linked, 2% BCB, surface rupture follows rippling and debris collects at the edges of the wear track after 12 scans; (c) cross-linked, 10% BCB, rippling is suppressed and only a small amount of debris is loosely distributed at edges of the wear track after ∼1000 scans; (d) cross-linked, 25%BCB, any changes to surface topography are only detected after ∼1500 scans and by averaging over 10 lines. (All AFM traces are recorded along the fast scan, and the unworn area of each image is used for flattening the data.)

removed from the surface. Quantification of nanowear requires a measure that captures the contributions from both viscoelastic rippling and pseudoplastic abrasion, while avoiding the complications of the classical methods discussed above. A common feature that can easily be identified regardless of the wear mode is the topographic deviation from the unperturbed surface. For this study, we define wear as the maximum topographical height change that is observed by AFM imaging. For example, the measure is provided by the maximum ripple height in the case of rippling (Figure 2a), by the pile-up height at the edge of the scan in the case of abrasion (Figure 2c/d), and by the larger of the two for mixed modes (Figure 2b). In our experience, the wear rate, given as the cumulative topographical height change divided by the total number of scans, turns out to be a useful means of monitoring the degree of wear, regardless of the wear mode. A typical wear diagram based on this and other studies[14−17] is pictured in Figure 3. Irrespective of the wear modes, the cumulative wear for a given sample evolves in a conical band with upper and lower wear boundaries that are separated by a factor of 3−5. Thus, irrespective of both the wear mode and the number of scans to which a particular sample is subjected, the uncertainty in the wear *rate* is within one-half to two-thirds of an order of magnitude. However, as the wear rate changes drastically with cross-linking (i.e., logarithmic scale in Figure 4), this uncertainty becomes insignificant. For any given sample, if wear initiates with rippling, the wear rate is reported as the average wear rate of several measurements covering all regions of Figure 3,

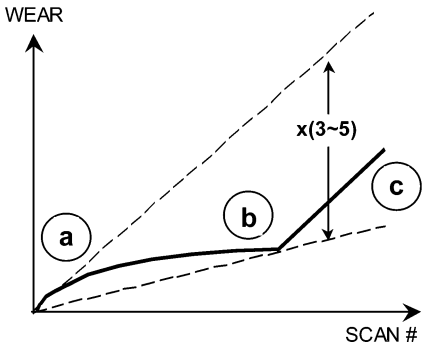

Figure 3. Schematic wear diagram: typical behavior represented by the solid line. The dominant wear mode changes during the course of the experiment, from (a) an initial rapid ripple formation to (b) an apparent static rippled state which ends abruptly with the onset of (c) rupture wear and abrasion. This evolution of wear modes leads to a long-term wear rate that is distributed between two extremes (given by the slopes of the dashed lines) separated by a factor of ~3−5.

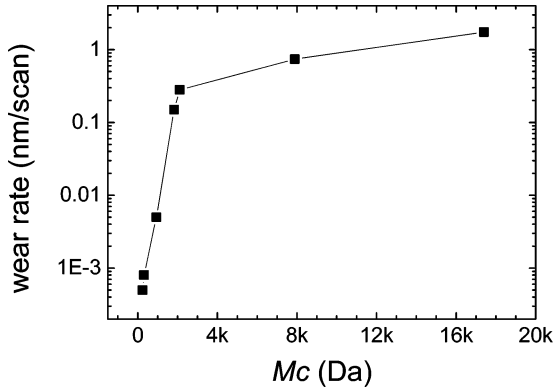

Figure 4. Impact of cross-link spacing on wear rate. Two wear regimes are separated by a critical molecular weight between cross-links, M_c. Below $M_{c,crit} = 2150 \pm 150$ Da, wear is highly sensitive to the cross-link density, while above 2150 Da, there is little wear dependence on M_c. The uncertainty level represents the intersecting domain defined by the root mean square variance of regression fits above and below $M_{c,crit}$.

typically after one to a few tens of scans. If no rippling occurs, the wear rate is determined from averaging measurements of region "c" in Figure 3, typically after hundreds to thousands of scans. Figure 2a is an example of ripple wear in regions "a" and "b", and parts b and c of Figure 2 are examples of abrasive wear in region "c".

The wear rate data are presented in Figure 4 as a function of the molecular weight between cross-links (M_c). The data span several orders of magnitude in both wear rate and M_c and are clearly divided into two regimes. Above a critical value $M_{c,crit} = 2150 \pm 150$ Da, wear depends roughly linearly on M_c (wear rate $\propto M_c^n$, $n = 0.7 \pm 0.4$). Below $M_{c,crit}$, a much stronger dependence on M_c is observed (wear rate $\propto M_c^n$, $n = 3.9 \pm 0.7$).

The results for $M_c > M_{c,crit}$ are similar to macroscopic wear studies on cross-linked polyethylene (PE),[18,19] where the wear volume depends linearly on M_c above $M_{c,crit} = 4500$ Da. The PE studies did not detect any wear below $M_{c,crit}$, which may result from the lack of local sensitivity due to large-area averaging over many asperities in macroscopic contacts. Macroscopic studies of a similar PS system cross-linked with divinylbenzene indicate the brittle fracture stress drops drastically below $M_{c,crit}$,[20] which is consistent with the decreasing pseudoplastic wear rate below $M_{c,crit}$ in Figure 4. However, the macroscopic experiment only revealed a brittle failure mode, with no ductile mode like the viscoelastic rippling we observe above $M_{c,crit}$. Macroscopic methods are insensitive to the nanoscopic dimensions of the ripples (10−20 nm amplitude, ~100 nm periodicity). The local sensitivity of our single nanoscopic probe reveals a duality of wear modes undetected on the macroscale. This finding is consistent with the variety of frictional dissipation mechanisms that have been identified with AFM polymer friction studies, e.g., dissipation through viscoelastic relaxation for surface sliding,[6,7] and dissipation through chain scission under plowing conditions.[8]

The abrupt change in wear rate at $M_{c,crit}$ implies the existence of a critical length scale, $\delta_{c,crit}$, which marks a shift in the dominant wear modes. When the spacing between cross-links exceeds $\delta_{c,crit}$, the material undergoes wear at a higher rate, which is weakly sensitive to changes in the cross-link spacing. Pronounced viscoelastic rippling is observed, which eventually gives way to pseudoplastic abrasive wear. In this scenario, sparse cross-linking does not appreciably contribute to the relaxational behavior of the entangled polymer network. A shift occurs to a different wear mode when the spacing between cross-links drops *below* $\delta_{c,crit}$. In this regime, the wear response of the material becomes extremely sensitive to changes in the cross-link spacing. No rippling is observed, and the abrasive wear rate decreases as the cross-link spacing becomes denser. This behavior suggests that the cross-links are spaced closely enough to interfere with the intrinsic behavior of the native polymer, hindering the dynamics of the underlying relaxation mechanisms.

The distance between cross-links, δ_c, can be estimated assuming that the polymer chain between cross-links behaves like an isolated chain of the same length. A critical distance between cross-links, $\delta_{c,crit}$, of 3 nm corresponds to $M_{c,crit} =$ 2150 Da, which consists of about 20 monomeric units, or six times the persistence length of the polymer chain (see refs 21−23 and Supplemental Information). Before addressing the intrinsic nature of the 3 nm critical cross-link spacing, it is necessary to evaluate the role of the dimensions of the probing tip: a hemisphere with a diameter of 20−30 nm. If a simple picture of tip penetration into the mesh of polymer chains is considered, a transition to a *low wear plateau* would be expected in Figure 4 as M_c approaches zero, where additional tightening of the cross-link spacing would have no further effect on tip penetration. This is not observed in our experiment. Furthermore, the 3 nm critical length is one order of magnitude smaller than tip dimensions. Hence, the transition in wear behavior at $M_{c,crit}$ in Figure 4 is not an artifact of the probe, but reflects an intrinsic material behavior. In this light, we consider how the cross-link spacing compares to other relevant material length scales.

Wear processes leading to the observed material displacements must involve either backbone *rupturing* (in the case

of abrasion via chain scission) or backbone *relaxation* (in the case of rippling or abrasion via chain pull-out). Relaxation processes in polymers occur at different length scales, from localized segmental relaxations covering a few repeat units to long-range modes involving the whole polymer chain, i.e., the so-called normal mode[24] which is not relevant in our cross-linked systems (see ref 25 and Supplemental Information).

The length scale of segmental motion during backbone relaxation, ξ_α, is generally discussed in terms of cooperatively rearranging regions or regions in space where the motion of an individual chain segment is contingent on the orchestrated or sequential motion of an ensemble of N_α surrounding segments, with $N_\alpha \sim \xi_\alpha^3$.[26] For many un-cross-linked polymers, ξ_α grows from the sub-nanometer scale in the melt to a *nondiverging* value of about 1−4 nm at T_g.[27−30] For polystyrene, ξ_α saturates at 3 nm when cooling from the melt.[31,32] Although cooperative motion is generally considered a process of the thermal glass transition, the relaxation process can also be operative in dissipating the external energy provided by the probe.

The correspondence of the experimental critical cross-link spacing, $\delta_{c,crit}$, of 3 nm with the 3 nm cooperation length, ξ_α, for backbone relaxation is striking, yet not unexpected. Considering that prior AFM scanning experiments on polystyrene have shown a correspondence of the length for frictional energy dissipation with the segmental cooperation length,[7] and given that the AFM tip-induced wear requires segmental relaxation, it is appropriate to attribute our observed $\delta_{c,crit}$ to cooperative segmental motion. For $\delta_c \gg \xi_\alpha$, the cross-links should not interfere with the natural backbone relaxation; hence, the observed wear characteristics are similar to the un-cross-linked polymer and exhibit a relatively weak dependence on the actual cross-link spacing. This behavior is portrayed in the shallow-sloped regime of Figure 4, where the concentration of cross-links is insufficient to restrain the rippling process and relatively higher wear rates are observed. On the other hand, when $\delta_c < \xi_\alpha$, cross-links within the domain of a cooperatively rearranging region directly interfere with the relaxation process. In this scenario, the cross-links are expected to impose constraints on the backbone mobility, effectively increasing the cooperation length. Consequently, the mobility constraints impede wear through viscoelastic relaxation; i.e., ripple formation is restricted by the enhanced chain connectivity. The relatively low wear rates in this regime are characterized by abrasive wear, indicative of *brittle* material response with dissipation predominantly through pseudoplastic modes.

The impact of confined backbone relaxation on the *shear* behavior discussed above is corroborated with the *normal* response of the same PS−BCB films to nanoindentation. The PS−BCB indentation hardness is represented in Figure 5 as the force required to produce a 0.5 nm deep indentation with an AFM tip. While the apparent hardness is strongly dependent on cross-link spacing below $M_{c,crit}$ of ∼2150 Da, it exhibits little dependence on cross-link spacing above $M_{c,crit}$. Compared to the un-cross-linked native polymer, the hardness for $M_c < M_{c,crit}$ is greater by a factor of up to 2.5,

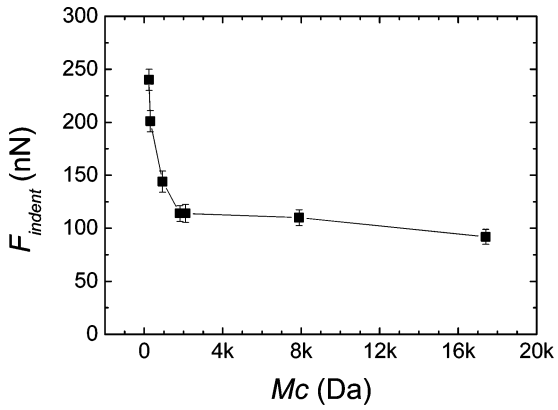

Figure 5. Impact of cross-link spacing on the hardness of the PS−BCB thin films: The minimum force needed to make a permanent 0.5 nm deep indentation, F_{indent}, is plotted versus the molecular weight between cross-links, M_c. (Note: for a given indentation geometry and penetration depth (i.e., equal contact area), the hardness is directly proportional to F_{indent}.)

whereas for $M_c > M_{c,crit}$, the hardness is within 25% of the un-cross-linked value.

The two domains in Figure 5 are explained by the interpretation presented above for wear, based on the interplay of δ_c and ξ_α. For $M_c < M_{c,crit}$ (i.e., $\delta_c < \xi_\alpha$), backbone mobility constraints imposed by the cross-links increase the cooperation length and impede viscoelastic relaxation. Hence, increasingly higher indentation loads are needed to initiate the pseudoplastic modes necessary to penetrate the surface. Above $M_{c,crit}$ in Figure 5, the cross-link spacing has little impact on the hardness. This coincides with $\delta_c \gg \xi_\alpha$ discussed above for wear; the cross-link concentration is insufficient to impede the intrinsic cooperation length for backbone relaxation. Backbone mobility is not appreciably confined at the higher M_c values, and the tip easily penetrates the surface.

In summary, we have observed the dependence of wear on segmental relaxation dynamics by tailoring the polymer synthesis with predetermined cross-linking levels. In doing so, we have identified means to reduce nanoscopic wear in a polymeric NEMS. Two wear regimes have been identified: (i) below a critical cross-link density a *ductile* wear mode exhibits weak dependence on the spacing between cross-links, and (ii) above a threshold cross-link density, a *brittle* wear mode becomes operative and the wear rate decreases rapidly with additional cross-linking. The threshold cross-link density that separates the two wear modes occurs at a critical segment weight of ∼2150 Da. This weight corresponds to a critical cross-link spacing of ∼3 nm, suggesting a competition between the cross-link spacing and the cooperation length for segmental backbone relaxation. When the spacing between cross-links falls below the cooperation length, constraints are imposed on the backbone mobility, essentially stiffening the material. Under these conditions, increased hardness and reduced wear are strongly correlated with cross-link spacing. If the concentration of cross-links is insufficient to interfere with natural backbone relaxation, the presence of cross-links has little impact on

the polymer response and the material behaves similarly to the un-cross-linked native polymer.

Critical to NEMS design is the ability to tailor nanoscale mechanical properties by controlling the internal degrees of freedom available for molecular relaxation. On this scale, *all* transport processes depend on the degrees of freedom available to molecular motion. A refined balance between molecular structure and device performance is essential in developing nanotechnologies.

Acknowledgment. We thank M. Despont and U. Drechsler for the cantilevers and tips and E. Harth for synthesis of the materials (NSF DMR 05-20415). P. Vettiger and J. Windeln are gratefully acknowledged for continuous support and stimulation. We thank A. Knoll and R. Schmidt for helpful discussions.

Supporting Information Available: Text on relation of the molecular weight to the radius of gyration, Kuhn length and persistence length, and *normal* mode relaxation as a function of molecular weight. This material is available free of charge via the Internet at http://pubs.acs.org.

References

(1) Wang, W.; Wang, Y.; Bao, H.; Xiong, B.; Bao, M. *Sens. Acuators, A* **2002,** *97*−*98*, 486-491.
(2) Vettiger, P.; et al. *IEEE Trans. Nanotechnol.* **2002**, *1*, 39−54.
(3) Bhushan, B.; Fuchs, H.; Hosaka, S. *Applied Scanning Probe Methods*; Springer: Berlin, 2004.
(4) Soh, H. T.; Wilder Guarini, K.; Quate, C. F. *Scanning Probe Lithography*; Kluwer Academic Publishers: Boston, MA, 2001.
(5) Schmidt, R.; Haugstad, G.; Gladfelter, W. L. *Langmuir* **2003**, *19*, 898−909.
(6) Sills, S.; Overney, R. M. *Phys. Rev. Lett.* **2003**, *91*, 095501.
(7) Sills, S.; Gray, T.; Overney, R. M. *J. Chem. Phys.* **2005**, *123*, 134902.
(8) Cappella, B.; Sturm, H.; Weidner, S. M. *Polymer* **2002**, *43*, 4461−4466.
(9) Washiyama, J.; Kramer, E.; Hui, C. *Macromolecules* **1993**, *26*, 2928−2934.
(10) Harth, E.; et al. *J. Am. Chem. Soc.* **2002**, *124*, 8653−60.
(11) The molecular weight of the cross-link agent (the weight of cross-linked BCB) was not included in the calculation of M_c but would merely shift the M_c values by 115 Da. For the pure polystyrene sample, M_c was identified with the entanglement molecular weight of 17 400 Da.
(12) Briscoe, B. J.; Evans, P. D.; Pelillo, E.; Sinha, S. K. *Wear* **1996**, *200*, 137−147.
(13) *Handbook of Mirco/Nanotribology*; Bushan, B., Ed.; CRC Press: Boca Raton, FL, 1995.
(14) Gotsmann, B.; Duerig, U. *Langmuir* **2004**, *20*, 1495−1500.
(15) Aoike, T.; Uehara, H.; Yamanobe, T.; Komoto, T. *Langmuir* **2001**, *17*, 2153−2159.
(16) Meyers, G. F.; DeKoven, B. M.; Seitz, J. T. *Langmuir* **1992**, *8*, 2330−2335.
(17) Schmidt, R.; et al. *Langmuir* **2003**, *19*, 10390−10398.
(18) Muratoglu, O. K.; Bragdon, C. B.; O'Connor, D. O.; Jasty, M.; Harris, W. H.; Gul, R.; McGarry, F. *Biomaterials* **1999**, *20*, 1463−1470.
(19) Wang, A. *Wear* **2001**, *248*, 38−47.
(20) *Polymer Toughening*; Arends, C. B., Ed.; Marcel Dekker: New York, 1994.
(21) Cotton, J. P.; et al. *Macromolecules* **1974**, *7*, 863−872.
(22) Elias, H.-G. *Macromoleküle*, 6th ed.; Wiley-VCH: Weinheim, 2001; Vol. 2.
(23) Solf, M. P.; Vilgis, T. A. *J. Phys. A*: *Math. Gen.* **1995**, *28*, 6655−6668.
(24) Schönhals, A.; Schlosser, E. *Phys. Scr.* **1993**, *T49*, 233−241.
(25) Abe, F.; Einaga, Y.; Yoshizaki, T.; Yamakawa, H. *Macromolecules* **1993**, *26*, 1884−1890.
(26) Donth, E. *J. Polym. Sci., Part B*: *Polym. Phys.* **1996**, *34*, 2881−2892.
(27) Ediger, M. D. *Annu. Rev. Phys. Chem.* **2000**, *51*, 99−128.
(28) Sillescu, H. *J. Non-Chryst. Solids* **1999**, *243*, 81−108.
(29) Tracht, U.; et al. *Phys. Rev. Lett.* **1998**, *81*, 2727−2730.
(30) Sillescu, H.; Bohmer, R.; Diezemann, G.; Hinze, G. *J. Non-Cryst. Solids* **2002**, *307*, 16−23.
(31) Donth, E. *J. Non-Cryst. Solids* **2002**, *307*−*310*, 364.
(32) Huth, H. Ph.D. Thesis, Universität Halle, 2001.

NL0520563